Supporting Information

Determination of phenolic compounds in estuary water and sediment by solid-phase isotope dansylation coupled with liquid chromatography-high resolution mass spectrometry

Wenxue Xu, Yufeng Hu, Minghuo Wu*, Enming Miao, Hao Zhou, Xuwang Zhang, Jingjing Zhan*

School of Ocean Science and Technology, Dalian University of Technology, Panjin 124221, China

*Corresponding authors:

Dr. Minghuo Wu

Email: wumh@dlut.edu.cn, Tel: +86-427-2631788

Dr. Jingjing Zhan

Email: jingjingzhan@dlut.edu.cn, Tel: +86-427-2631789

17 Table S1. Structure and theoretical mass-to-charge ratio (m/z) of the phenols.

Analyte	Structure	Theoretical m/z		
		Un-labeled $[M-H]^-$	D0-labeled $[M+H]^+$	D6-labeled $[M+H]^+$
phenol	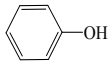	93.03459	328.10019	334.13785
resorcin	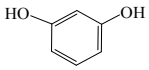	109.0295	344.09511	350.13277
p-cresol	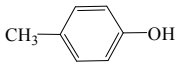	107.05024	342.11584	348.1535
2,4-DCP	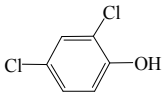	160.95564	396.02225	402.05991
3,5-DMP	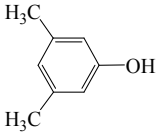	121.06589	356.13149	362.16915
o-NP	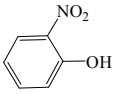	138.01967	373.08527	379.12293
p-NP	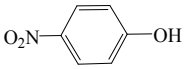	138.01967	373.08527	379.12293
4-C-3-MP	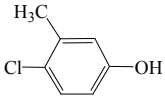	141.01127	376.07687	382.11453
o-CP	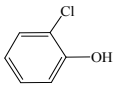	126.99562	362.06122	368.09888
TCS	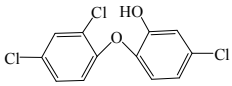	286.94389	522.00949	528.04715
BPA	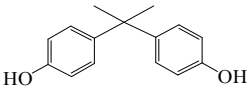	227.10775	695.2244	707.29973
BPB	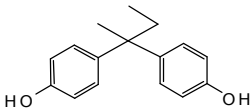	241.12340	709.24005	721.31538
BPE	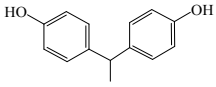	213.09210	681.20875	693.28408

BPF	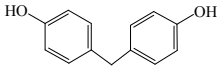	199.07645	667.1931	679.26843
BPZ	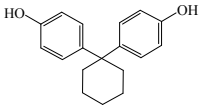	267.13905	735.2557	747.33103

22 Table S2. The linearity (R^2) and reproducibility (RSD) for the analysis of spiked pond

23 water samples at phenols concentration of 0.05- 20 μg/L except phenol and resorcin.

Analyte	R^2	RSD (%, n=3)						
		0.01	0.05	0.1	1	5	10	20
phenol	0.9998	-	4.8	5.4	3.7	6.8	9.1	7.1
resorcin	0.9917	-	10.3	8.5	9.0	8.7	9.0	6.1
p-cresol	0.9978	6.1	4.9	3.6	1.4	4.2	5.1	3.0
2,4-DCP	0.9974	4.1	3.9	5.3	2.3	3.1	5.2	2.3
3,5-DMP	0.9979	3.9	5.6	4.2	2.5	2.8	5.1	5.5
o-NP	0.9926	6.5	4.9	6.2	3.9	4.2	5.0	7.6
p-NP	0.9914	5.3	3.6	5.3	2.1	3.5	5.2	7.5
4-C-3-MP	0.9928	5.9	4.4	6.3	5.0	3.8	4.1	9.5
o-CP	0.9997	3.1	2.9	3.5	4.6	5.2	5.0	4.6
TCS	0.9976	2.8	3.0	3.8	4.1	3.6	5.0	5.1
BPA	0.9977	5.9	5.1	5.7	2.3	4.5	5.2	6.9
BPB	0.9978	5.1	6.3	3.7	2.3	1.8	5.1	6.1
BPE	09983	4.2	6.1	4.7	3.6	2.2	5.1	7.1
BPF	0.9996	4.3	5.7	2.9	6.0	3.8	5.0	6.4
BPZ	0.9987	6.6	4.7	5.8	3.4	4.0	5.0	5.5

24

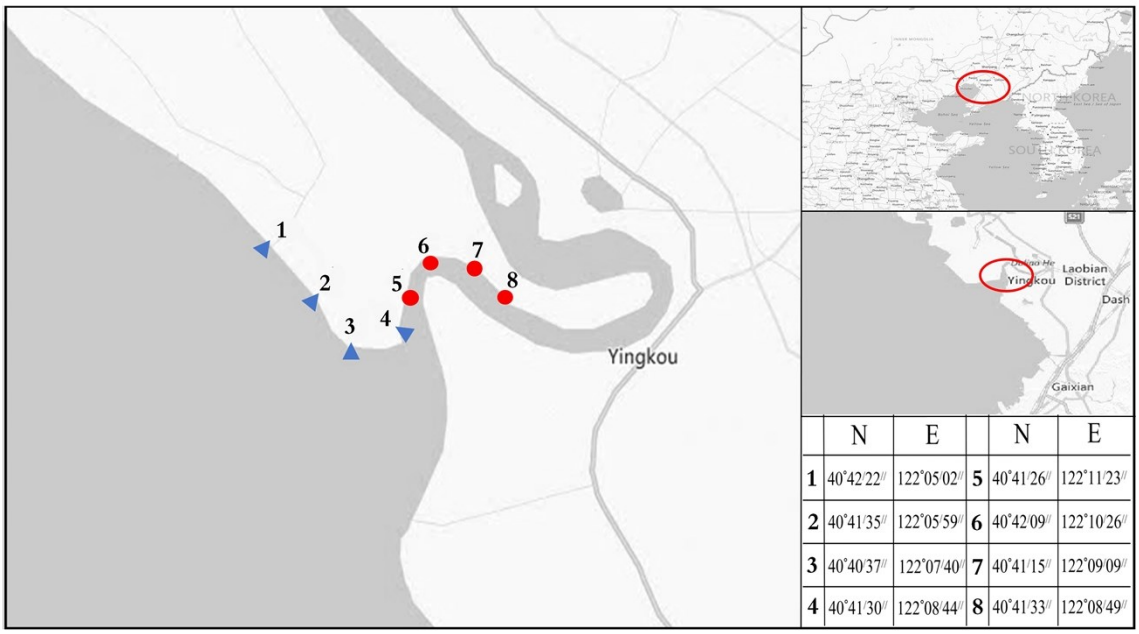

	N	E		N	E
1	40°42′22″	122°05′02″	**5**	40°41′26″	122°11′23″
2	40°41′35″	122°05′59″	**6**	40°42′09″	122°10′26″
3	40°40′37″	122°07′40″	**7**	40°41′15″	122°09′09″
4	40°41′30″	122°08′44″	**8**	40°41′33″	122°08′49″

Fig. S1. Illustration of the sampling sites along the estuary.

Adapted from The National Geologic Map Database; U.S. Geological Survey, 2019.

28 **Synthesis and characterization of the magnetic materials**

29 The magnetic-HLB for MSPE was synthesized according to our previously reported
30 method (details were presented in SI).[1-2] In detail, HLB material (0.2 g), $FeSO_4$ (1.5 g) and
31 $FeCl_3$ (1.6 g) were mixed in water (20 mL), and heated to 60 °C. And then, the mixture
32 was dropwise added into an ammonia solution (45 mL, 3.0 mol/L) and ultrasonicated at 60
33 °C for 30 min. After reaction, the solution was cooled to room temperature. The resultant
34 magnetic HLB material (M-HLB) was collected and washed with water repeatedly to
35 neutral pH, and dried in a vacuum oven at 60 °C. The micro morphologies of HLB and M-
36 HLB were characterized by scanning electron microscope (SEM), and the elemental
37 composition was investigated by energy dispersive spectrometry (EDS). The valence state
38 of Fe was examined by X-ray diffraction (XRD). The specific surface area for both
39 materials (HLB and M-HLB) was measured by Brunauer-Emmett-Teller (BET).

40 **Characterization of the magnetic materials**

41 From the SEM images of M-HLB, it was found that there were considerable amount
42 of nano-sized particles attached on the micro spheres (Fig. S2). The results from EDS (Fig.
43 S3) revealed the existence of Fe element in these particles, which were further confirmed
44 as Fe_3O_4 by the XRD results (XRD patterns corresponding to the cubic inverse spinel
45 structure of Fe_3O_4 at [220], [311], [400], [422], [511], [440] and [533], which were
46 observed at 30.18°, 35.5°, 43.3°, 53.8°, 57.2°, 62.7° and 74.4°, respectively. Fig. S4). From
47 the BET analysis results, a lowered specific surface area of 68.848 m^2/g for M-HLB was
48 observed (690.5094 m^2/g for the pristine HLB, Fig. S5), and the pore volume at diameter

of <5 nm decreased dramatically, which was owning to the blocking by magnetic particles.[2]

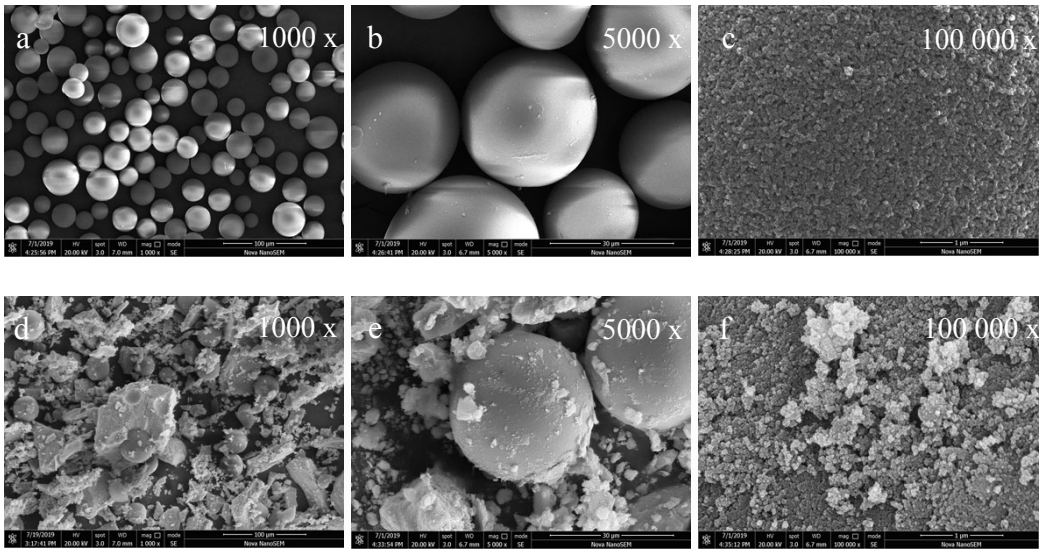

Fig. S2. SEM images of HLB (a, b, c) and M-HLB (d, e, f) with different magnification.

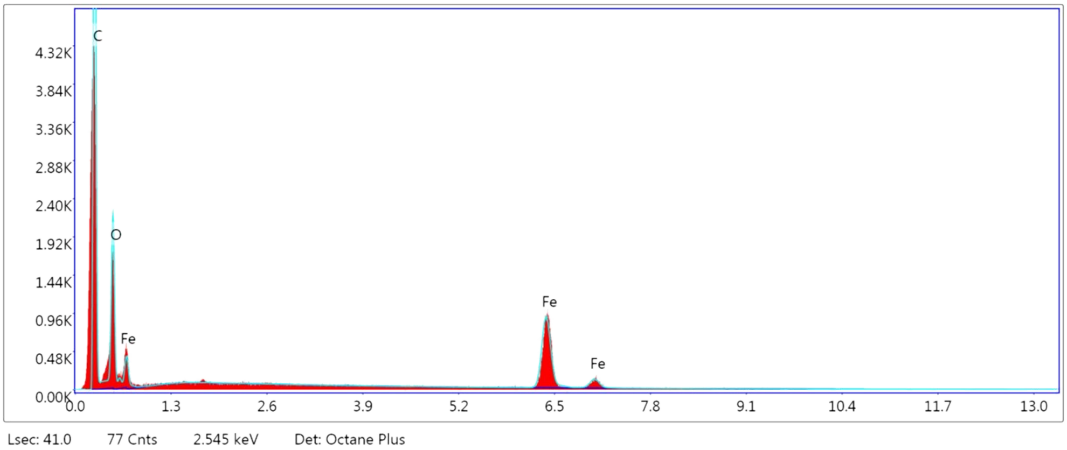

Fig. S3. Energy dispersive spectrometry (EDS) analysis of the M-HLB.

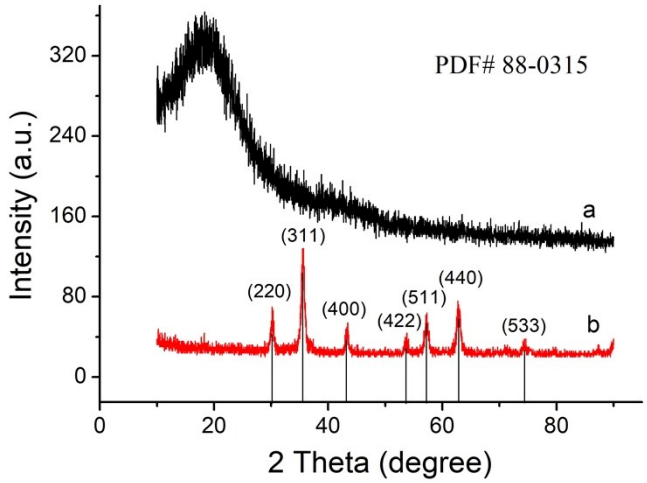

Fig. S4. X-ray diffraction (XRD) patterns of a) HLB and b) M-HLB.

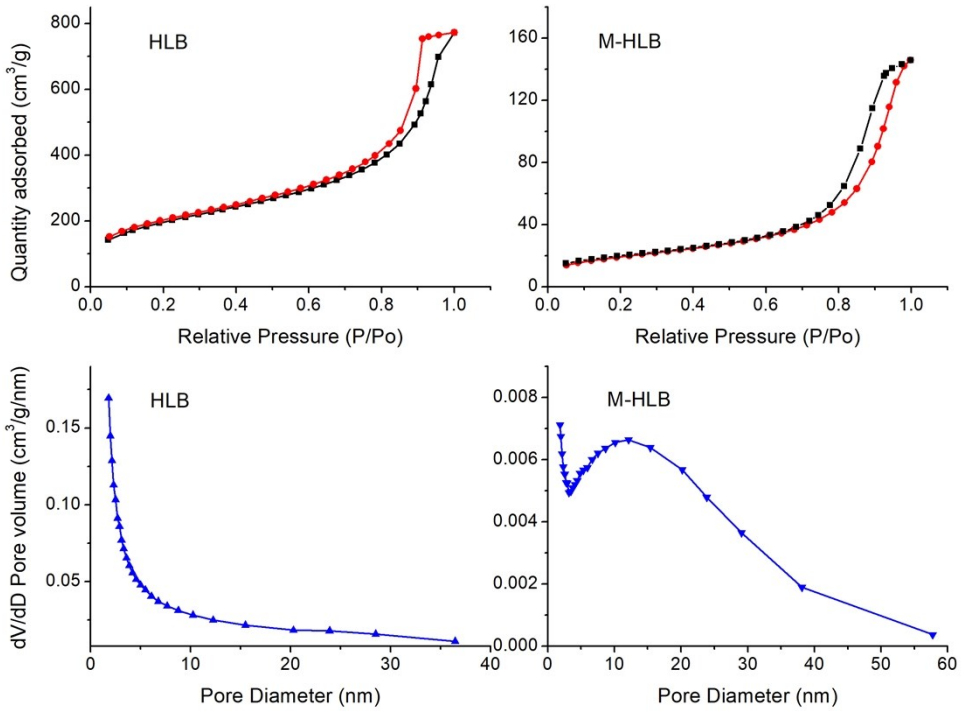

Fig. S5. The nitrogen adsorption-desorption isotherm and pore size distribution plot of HLB and M-HLB.

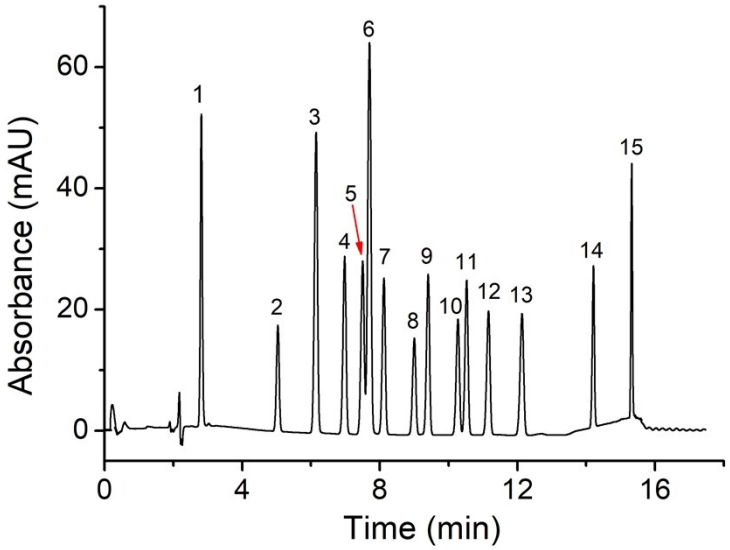

Fig. S6. Separation of the tested phenols on LC-UV.

Analytes: 1) resorcin; 2) phenol; 3) p-NP; 4) p-cresol; 5) BPF; 6) o-CP;7) o-NP; 8) BPE; 9) 3,5-DMP; 10) BPA; 11) 4-C-3-MP;12) 2,4-DCP; 13) BPB; 14) BPZ; 15) TCS. Each at 15 mg/L.

The LC-UV analysis of phenols were performed on a binary pump system equipped with an autosampler, a column oven, a C18 (Hypersil BDS, 5 μm × 4.6 mm × 250 mm) and a UV detector (EClassical 3100, Elite, Dalian, China). Mobile phase: A) water containing 0.1% FA; B) ACN containing 0.1% FA. LC gradient: 0-6.0 min, 30-50% B; 6.0-9.0 min, 50-60% B; 9.0-11.0 min, 60% B; 11.0-13.0 min, 60-95% B; 13.0-15.0 min, 95% B; 15.0-15.1 min, 95-30% B and 15.1-16.0 min, 30% B. Other conditions: flow rate, 1.5 mL/min; injection volume, 20 μL; column oven temperature, 50 °C; detection wavelength, 280 nm.

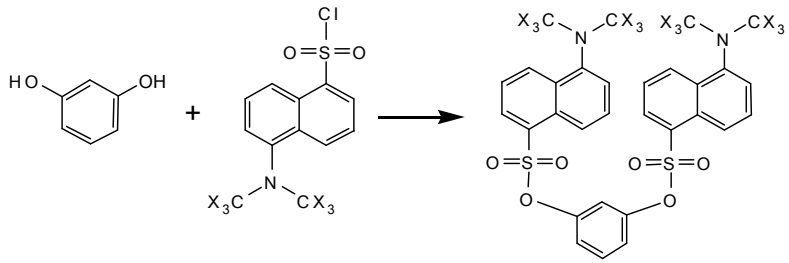

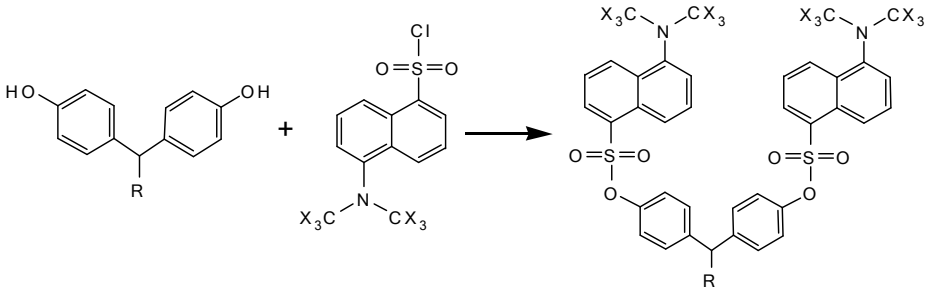

Fig. S7. Illustration of the dansylation for the phenols with two labeling sites.

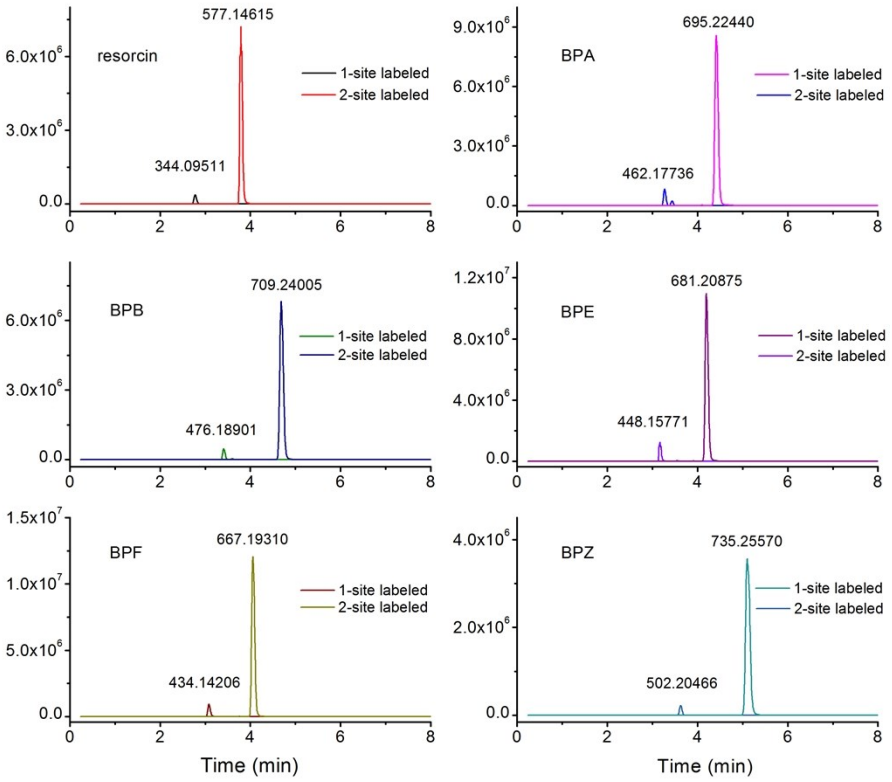

Fig. S8. The XICs of the dansylated phenols containing two labeling sites.

83 **Optimization of the MSPE and solid-phase labeling**

84 The amount of adsorbent was briefly optimized (15, 30 and 40 mg) with a solution 10
85 mg/L (10 mL). The residuals of phenols in the solutions after adsorption were analyzed by
86 LC-UV. As shown in Fig. S9, 30 mg was selected as higher mount (40 mg) provided
87 limited improvement in adsorption.

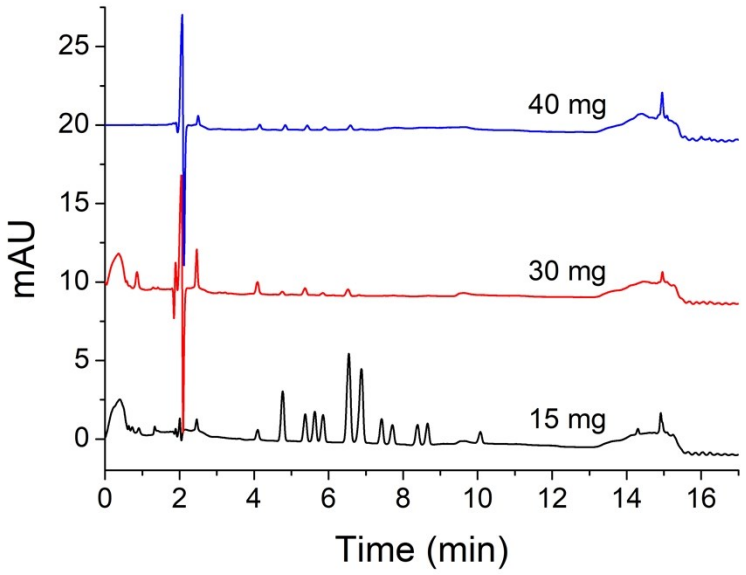

88

89 Fig. S9. The residual of phenols in the solution after adsoption with different amount
90 of M-HLB in the MSPE.

91 For the optimization of water content in reaction buffer, the ratio of water to ACN
92 from 3:1-3:3 (v/v) were performed at pH 10.08, Dns-Cl 100 mg/L, temperature 40 °C,
93 reaction time 60 min. For the optimization amount of Dns-Cl at the concentration from 20
94 to 100 mg/L were performed at the ratio of water to ACN 1:1 (v/v), pH 10.08, temperature
95 40 °C and reaction time 60 min. For the optimization reaction temperature, 30 to 70°C were
96 performed at the ratio of water to ACN 1:1(v/v), Dns-Cl 100 mg/L, pH 10.08, Dns-Cl 100

97 mg/L, and reaction time 60 min. The pH range of 8.77-10.57 were optimized at the ratio
98 of water to ACN 1:1(v/v), Dns-Cl 100 mg/L, temperature 40 °C, and reaction time 60 min.
99 The reaction solvent volume from 0.2 to1.0 mL were tested at the ratio of water to ACN
100 1:1(v/v), Dns-Cl 100 mg/L, temperature 40 °C, pH 9.72 and reaction time 60 min. The
101 reaction time from 5 to 60 min were compared at the ratio of water to ACN 1:1(v/v), Dns-Cl
102 100 mg/L, temperature 40 °C, pH 9.72 and reaction solvent volume 0.2 mL. After reaction,
103 D6-dansylated phenols were mixed with each reaction solution, and analyzed by LC-
104 HRMS. The optimization results were evaluated based on the peak area ratios of the D0 to
105 D6-dansylated phenols.

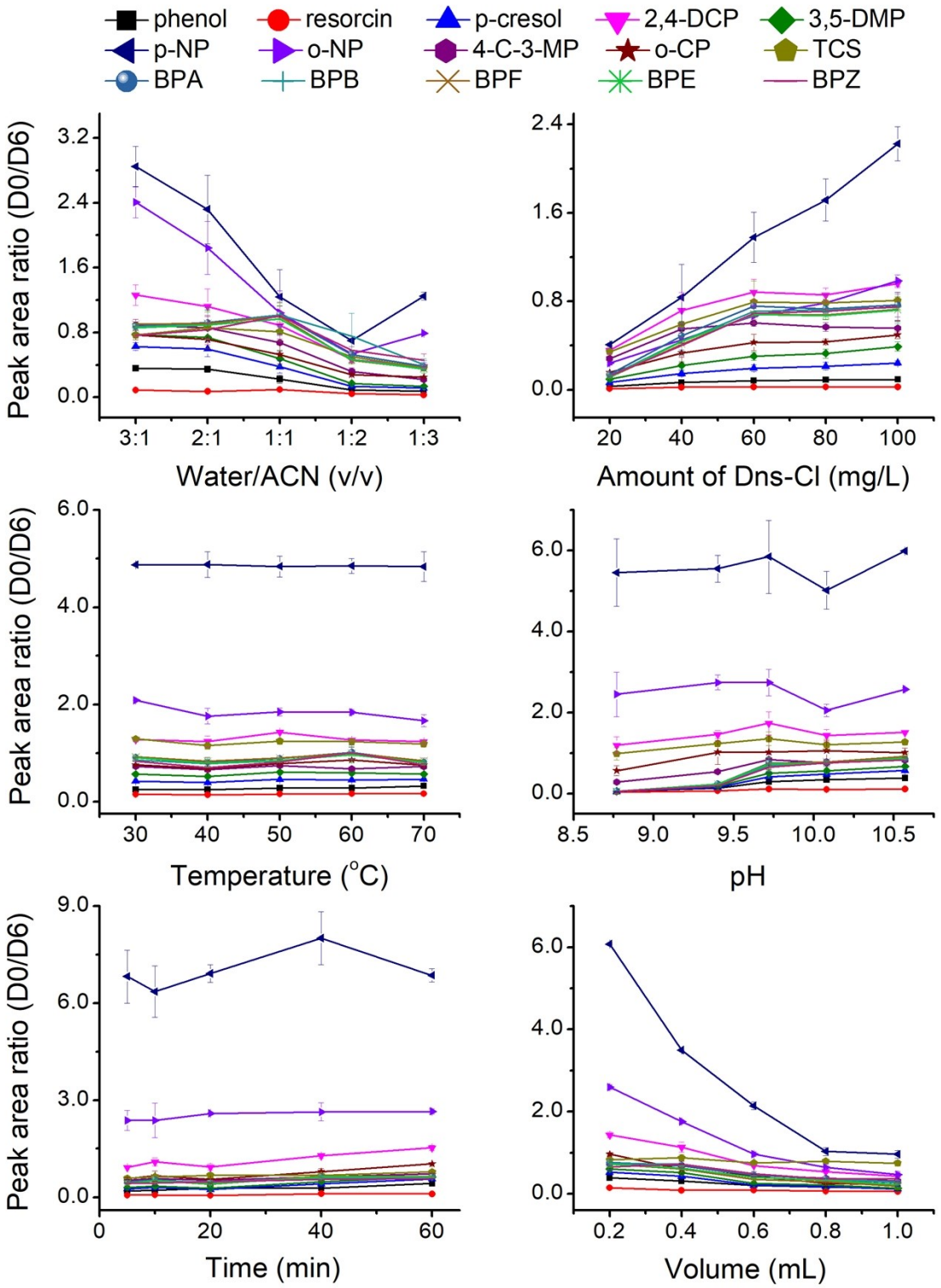

Fig. S10. Optimization of the solid-phase labeling conditions.

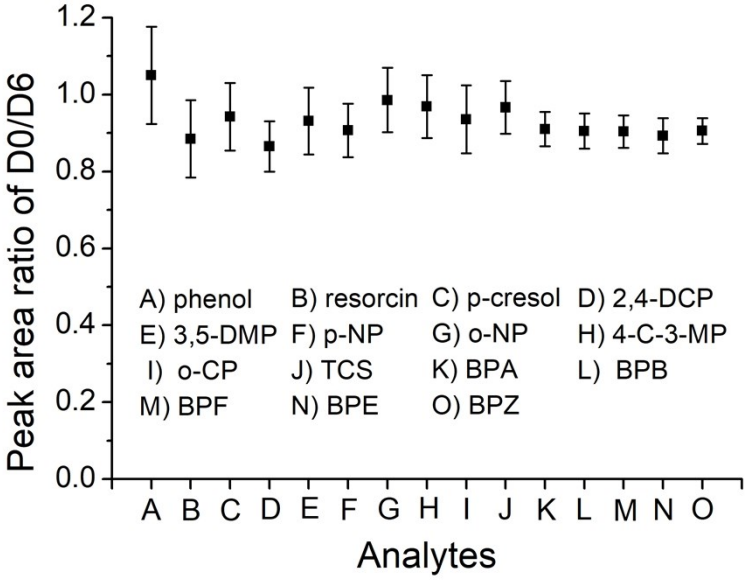

Fig. S11. Signal-response ratios of D0- to D6-dansylated phenols.

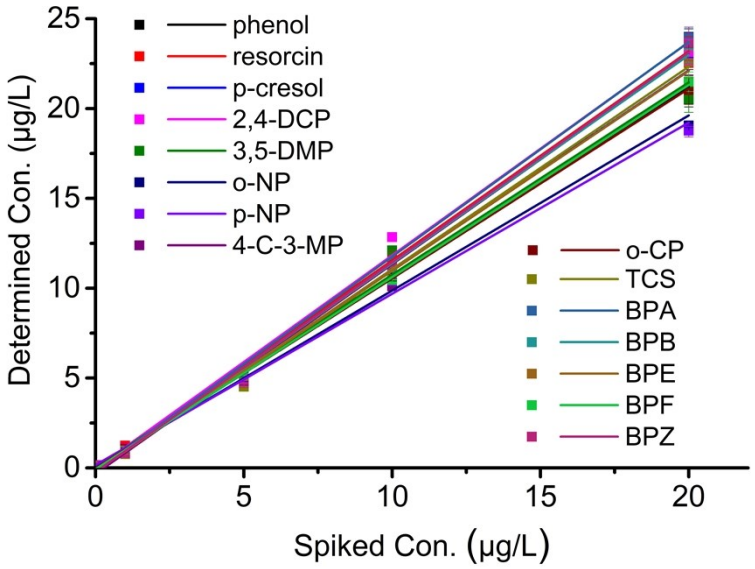

Fig. S12. Linear quantification curves of the method.

Concentration at 0.01-20 μg/L, except phenol and resorin at 0.05-20 μg/L.

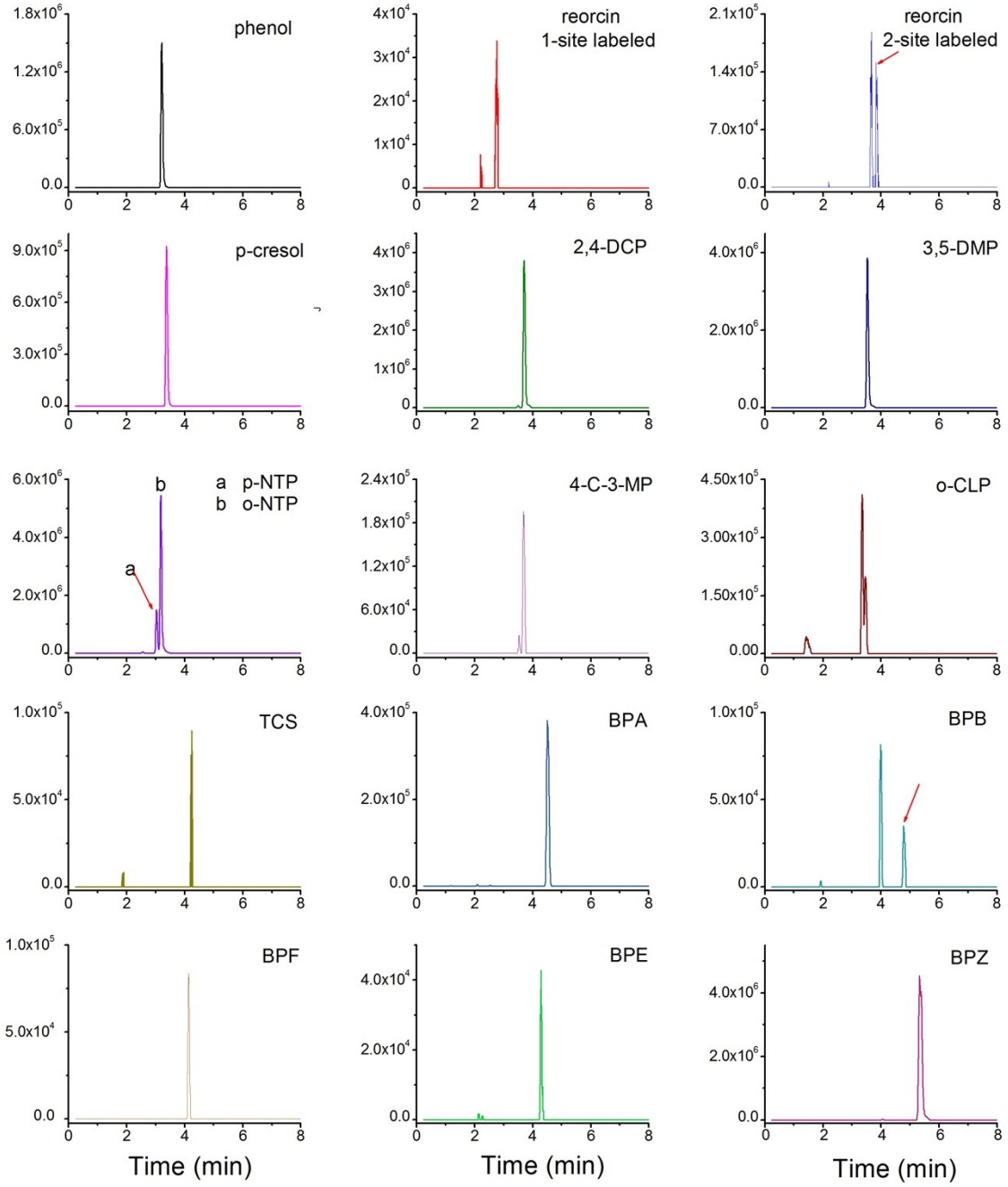

Fig. S13. The XICs of phenols determined in the water sample (Site 1).

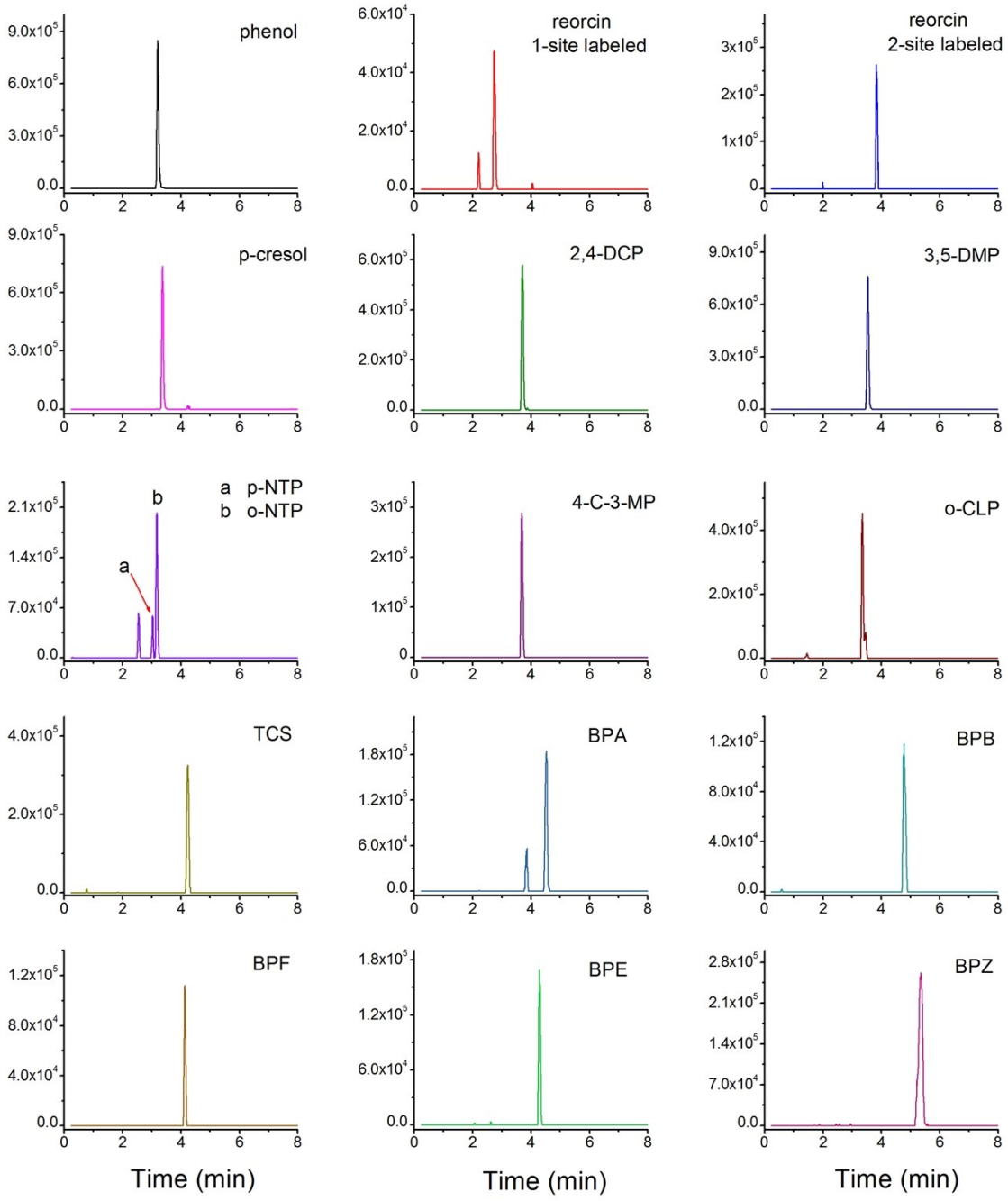

Fig. S14. The XICs of phenols determined in the sediment sample (Site 5).

118 **Reference**

119 1. L. Fu; H. Zhou; E. M. Miao; S. W. Lu; S. Y. Jing; Y. F. Hu; L. J. Wei; J. J. Zhan; M.
120 H. Wu, Functionalization of amino terminated carbon nanotubes with isocyanates for
121 magnetic solid phase extraction of sulfonamides from milk and their subsequent
122 determination by liquid chromatography-high resolution mass spectrometry. *Food*
123 *Chem.* **2019,** *289*, 701-707.
124 2. E. M. Miao; N. Z. Zhang; S. W. Lu; Y. F. Hu; L. Fu; H. Zhou; J. J. Zhan; M. H. Wu,
125 Solid phase "on-situ" quadraplex isotope dimethyl labeling for the analysis of
126 biogenic amines in beers by liquid chromatography-high resolution mass
127 spectrometry. *J. Chromatogr. A,* **2020**, doi.org/10.1016/j.chroma.2019.460712